26th ABCM International Congress of Mechanical Engineering
November 22-26, 2021. Florianópolis, SC, Brazil

COB-2021-0435
MULTI-MATERIAL TOPOLOGY OPTIMIZATION WITH STRESS CONSTRAINTS

Rodrigo Reis Amaral
Federal University of Rio Grande do Sul, Av. Sarmento Leite, 425, sala 202, 2º. Andar, 90050-170, Porto Alegre, RS, Brazil
rodrigo_amaral_23@hotmail.com

Herbert Martins Gomes[b]
Federal University of Rio Grande do Sul, Av. Sarmento Leite, 425, sala 202, 2º. Andar, 90050-170, Porto Alegre, RS, Brazil
herbert@mecanica.ufrgs.br

Abstract. *Designing engineering systems can be a complex process. Assumptions must be made to develop realistic models that can be subjected to mathematical analysis by the available methods. Structural optimization is a fusion in the areas of engineering, mathematics, science, and technology that has the objective to achieve the best performance for a structure. In this article, a linear analysis of a topologically optimized beam that uses concrete and steel in its composition will be presented. For this, a topological optimization procedure will be developed using the method Evolutionary Structural Optimization for problems that maximize the compliance of the structure. Failure criteria, such as that of Ottersen and von Mises, will be used for concrete and steel, respectively. With the criteria defined, it is possible to indicate which portion of the material is inefficient in parts of the structure, i. e., ideally, the stress in every part of the structure should be close to the same safe level. This concept leads to a rejection criterion based on the local stress level, where the low-stressed material is considered under-utilized. Regarding the numerical results, new topologies of beam structure using two nonzero materials and with void and two nonzero materials are presented.*

Keywords: *Reinforced concrete structure, Heterogeneous structure, Stress-based topology optimization*

1. INTRODUCTION

The construction industry represents a major environmental impact, as for every 1000 kg of cement produced, 900 kg of $CO2$ is released into the environment – representing an annual emission of 5% of carbon dioxide (Amir, 2013). Observing these values, it is clear the need to seek new methodologies that enable the design of reinforced concrete structures with a greater degree of slenderness, that is, that uses a relatively small amount of material without entering the service limit state.

One of the most effective ways to tackle the challenge of lightweight structures is through a combination of multi-material design and topology optimization. Thus, the properties of the structure can be adjusted by controlling the composition of the material. The design domain analysis consists of determining the behavior of the structure as a function of the applied load and boundary conditions, being most commonly performed by the Finite Element Method. In the algorithm, this optimization is handled in phases, so that the volume fraction for each of the phases needs to be specified by the designer. This gives the required volume fraction value of each material phase in the final design domain. (Querin et al., 2017).

Several techniques based on topology optimization have been used by researchers in recent decades, such as the Solid Isotropic Material with Penalization (SIMP) (Bendsøe & Sigmund, 2003), Level-Set Method (LSM) (Sethian and Wiegmann, 2000), and Bidirectional Evolutionary Structural Optimization (BESO) (Huang & Xie, 2010). Among the researches that address the subject of optimization in structural analysis with multi-material, it is possible to mention Wang and Wang (2004) for employing a multi-phase level-set model in a multi-material criteria domain. This model would eliminate the need for material interpolation or phase mixing of a homogenization-based approach. The multi-phase model automatically avoids the problem of overlap between material phases of a conventional level-set approach. The proposed multi-phase approach naturally lends itself to more general optimal design problems involving multi-physics such as optimization of heterogeneous materials and/or graded materials.

Lund (2009) presents the development of buckling topology optimization of laminated multi-material composite shell structures using the Discrete Material Optimization approach. The multi-material design problems may be solved together with the orientational problem associated with fiber-reinforced materials. The examples have illustrated the potential of the Discrete Material Optimization developed for simultaneous material selection and orientation. Results indicated that the optimization method may not yield full convergence everywhere in the design domain.

Luo et al. (2012) present a three-phase topology optimization model and an effective solution procedure to generate optimal material distributions for complex steel-concrete composite structures. The algorithm's objective is to minimize the total material cost (or mass) while satisfying the specified structural stiffness requirements and concrete strength constraints. Based on the Drucker–Prager criterion for concrete yield behavior, the extended power-law interpolation for material properties and a cosine-type relaxation scheme for Drucker–Prager stress constraints are adopted. The obtained solutions are compared with the designs obtained by using conventional topology optimization models. It is shown that the proposed steel-concrete composite designs are more economical than the pure steel counterparts when the same stiffness needs to be achieved. The comparison also reveals that it may be dangerous to design steel-concrete composites without considering the concrete strength constraints.

Tong et al. (2016) present a topology optimization with multi-materials under the mass constraint and the conditions of steady-state temperature and mechanical loading. In the study, the mass constraint is formulated using the linear form of the design variables to automatically balance the spatial distributions of the materials over the specific design domain. The results indicated that, due to the presence of thermal stress loads, numerical tests highlight that non-uniform initial weighting in the interpolation scheme might be more advantageous than the uniform initial weighting in obtaining the optimum solution.

Zhang and Chi (2020) present a general and efficient multi-material topology optimization framework considering hyper- elasticity with many local constraints, which enables flexible control of the design's local features. The proposed framework can effectively distribute multiple candidate materials described by distinct constitutive models according to their respective nonlinear behaviors, and efficiently handle a flexible setting of volume constraints (global or local). Their framework offers a paradigm for the computational design and optimization of nonlinear composite metamaterials and structures.

Recently, Li and Xie (2021) developed an algorithm based on the bi-directional evolutionary structural optimization (BESO) technique for rearranging the material suitable for tension in the tensile zone and the material suitable for compression in the compressive zone. The results indicated that the final designs obtained by topology optimization with single and with multiple materials show that the proposed method has an advantage in material savings. Also, the comparing of topologically optimized multi-material obtained with different mesh densities demonstrates the mesh independence of the method.

In addition, experimental researches addressing topological optimization applied to plain concrete with improved performance in the elastic range, Jewett and Carstensen (2019), and reinforced concrete structures, Liu et al. (2020), can also be found in the literature. They demonstrate the feasibility of the application of the method for topologically optimized concrete structures with built prototypes.

In this paper, a multi-material topology optimization based on Evolutionary Structural Optimization (ESO) applied for reinforced concrete structures is presented. The algorithm used in this study was adapted from de Marco (2018). Unlike the original code, Ottosen's 4-parameter criterion is considered in the analysis to determine the concrete material failure. Thus, a comparison between the Ottosen and Drucker-Prager criteria (originally used by de Marco, 2018) will be performed to determine the final topology of a loaded corbel jointed to a column structure. In addition, a comparison between the final results of methodologies will be carried out to demonstrate the feasibility of the ESO method for reinforced concrete structures when compared with a result found in the literature. Results indicate that it is possible to obtain lighter structures and still comply with the material failure criteria.

2. TOPOLOGY OPTIMIZATION

2.1 Multimaterial Topology Optimization ESO

Structural topology optimization is a rapidly developing field in computational mechanics. In standard approaches, topology optimization is used to adjust some design parameters to achieve some objectives, such as minimum volume, without violating certain constraints that usually is found in engineering problems. According to Huang and Xie (2010), for the stiffness optimization of structures with multiple materials, it is assumed that the elasticity moduli of different materials (n) are ranked $E_1, E_2, \cdots, E_j, \cdots, E_n$ ($E_1 > E_2 > \cdots E_j \cdots > E_n$) respectively and the prescribed volume for each material is V_j^*. In this way, the corresponding optimization problem can be stated as

$$\begin{gathered} \text{Minimize } \boldsymbol{C} = \frac{1}{2}\boldsymbol{f}^T\boldsymbol{u}, \\ \text{Subject to } V_j^* - \sum_{i=1}^{N} V_i x_{ij} - \sum_{i=1}^{j-1} V_i^* = 0 \;\; (j = 1, 2, \cdots, n-1), \\ x_{ij} = \begin{cases} x_{min} \text{ for E} \geq \text{E}_\text{j} \\ 1 \text{ for } E \leq E_j \end{cases}, \end{gathered} \tag{1}$$

where N is the number of finite elements, V_j^* is the prescribed volume to reach during the optimization process, $\boldsymbol{C}$ is the objective function of the compliance to be minimized and x_{ij} is the material density of the i^{th} element of the j^{th} material

used in the material interpolation scheme. So, based on the design parameters x_{ij}, the elemental material Young modulus is defined as:

$$E(x_{ij}) = x_{ij}^{p} E_j + (1 - x_{ij}^{p}) E_{j+1}, \tag{2}$$

where p is the penalty exponent, usually chosen as $p = 3$.

As for the addition or removal of the elemental material by the ESO method, this occurs through numerical analysis of the sensitivity number – Equation (3). Thus, for the case of a standard ESO multi-material, the sensitivity number for stiffness optimization is expressed as a function of the elemental compliance, an inverse measure of the importance of the element to the overall stiffness of the member, as described in Huang and Xie, 2010.

$$\alpha_{ij} = \begin{cases} \frac{1}{2}\left[1 - \frac{E_{j+1}}{E_j}\right] \boldsymbol{u}_i^T \boldsymbol{K}_i^j \boldsymbol{u}_i \ \text{ for materials } 1, \cdots, \text{j} \\ \frac{1}{2} \frac{x_{min}^{p-1}(E_j - E_{j+1})}{x_{min}^{p} E_j + (1 - x_{min}^{p}) E_{j+1}} \boldsymbol{u}_i^T \boldsymbol{K}_i^{j+1} \boldsymbol{u}_i \ \text{ for materials j} + 1, \cdots, n \end{cases}, \tag{3}$$

where $\boldsymbol{K}_i^j$ and $\boldsymbol{K}_i^{j+1}$ denote the elemental stiffness matrices calculated using $\mathrm{E_j}$ and $\mathrm{E_{j+1}}$ respectively. It should be noted that the sensitivity number α_{ij} is defined in the whole design domain even though it is only used for making adjustments between materials j and $j + 1$. When dealing with non-homogeneous materials, like reinforced concrete, this sensitivity can be changed to account for surface failure-based criteria related to the local stress states, as a matter of representing the importance of the element to the overall member's strength.

According to de Marco (2018), to avoid numerical instabilities, as the checkerboard pattern, and to ensure mesh independence, it is adopted a filtering scheme to average sensitivity numbers of neighboring elements and smooth out the sensitivity numbers field. The technique uses the average sensitivity numbers of connected elements to define the nodal sensitivity numbers, i.e., all nodes inside the circular domain with a radius r_{min} concur to the calculation of the α_{ij} with different weights in the sum process. The optimization is carried on in an iterative process, which is stopped when the values of the objective function (e.g. compliance) are converging to a stable value, i.e., it is set a convergence criterion expressed as

$$Error = \frac{\left|\sum_{l=1}^{L} C_{k-l+1} - C_{k-L-l+1}\right|}{\sum_{l=1}^{L} C_{k-l+1}} < 0.001 = 0.1\% \,. \tag{4}$$

3. MATERIAL MODELLING

Both failure surface criteria presented in this topic, for concrete and steel materials, are considered as constraints to be added to the objective function presented in Equation (1).

3.1 Concrete

A realistic solution for a structural problem involving concrete depends in large part on the choice of an appropriate constitutive model. The mechanical response of the concrete is complex and it seems unlikely that any phenomenological approach would be able to explain all the possible variations of the material's behavior. The four parameters failure surface, proposed by Ottosen (1977), for example, is a criterion adequate to explain the behavior for short-time loading applied in the concrete material. It involves the stress invariants I_1 and J_2 , and the loading angle θ in its equation (Oliveira et al., 2020). Thus, Ottosen's criterion can be expressed as

$$f(I_1, J_2, \theta) = c_1 J_2 + \lambda J_2^{0.5} + c_2 I_1 - 1 = 0, \tag{5}$$

where λ is a function of $\cos 3\theta$:

$$\lambda = \begin{cases} k_1 \cos\left[\frac{1}{3}\cos^{-1}(k_2 \cos 3\theta)\right] \ \text{ for } \cos 3\theta \geq 0 \\ k_1 \cos\left[\frac{\pi}{3} - \frac{1}{3}\cos^{-1}(-k_2 \cos 3\theta)\right] \ \text{ for } \cos 3\theta \leq 0 \end{cases}, \tag{6}$$

where $\cos 3\theta = 3\sqrt{3}J_3/(2\sqrt[2]{J_2^3})$ and c_1, c_2, k_1 and k_2 are constants defined by CEB-FIP (2010), a function of f_{cm} and f_{tm}.

According to Chen (1988), the model encompasses several earlier models as special cases, e.g, the von Mises model for $c_1 = c_2 = 0$ and $\lambda =$ constant and the Drucker-Prager model for $c_1 = 0$ and $\lambda =$ constant.

Regarding the Drucker-Prager criterion, according to Oliveira et al. (2020), it requires that the plastic yield point occurs when the second invariant of the deviatoric stress tensor J_2 and the hydrostatic pressure reaches a critical combination. The function that models the Drucker-Prager criteria for the stress state is given by:

$$f(\sigma, \varepsilon_p) = \alpha I_1 + J_2^{0.5} - k = 0, \tag{7}$$

where α and k are positive material constants function of f_{cm} and f_{tm}.

3.2 Reinforcing bars

According to Xie and Steven (1997), for the modeling of reinforcing bars made of steel (isotropic material), the von Mises stress criterion is adequate to represent the yielding of this material. The model considers that yielding of a ductile material begins when the second invariant of deviatoric stress J_2 reaches a critical value (f_y). Thus, for plane stress problems the von Mises stress σ_{vm} is defined as

$$f(\sigma, f_y) = \sqrt{J_2} - f_y = \sqrt{\sigma_x^2 + \sigma_y^2 - \sigma_x\sigma_y + 3\tau_{xy}^2} - f_y = 0. \tag{8}$$

Also, when working with the ESO method, it is necessary to be careful about transitioning from one failure criterion to another. According to de Marco (2018), a gradual transition in the optimization loop is introduced through a linear interpolation of sensitivity numbers to avoid, for example, placing the concrete in tensioned regions. Moreover, additional geometrical constraints are applied, to ensure a set minimal distance between steel and outer boundaries, i.e., concrete cover, and to ensure optimal angle preservation for steel members found during optimization.

4. RESULTS AND DISCUSSIONS

In this topic, two topology optimization problems will be presented. For the first example, a comparison between the failure models for the concrete material will be carried out. A comparison between the Ottosen and Drucker-Prager models will be made to assess how much this choice made by the designer can influence the final topology for the case of a loaded corbel jointed to a column taken from de Marco (2018). In this example, numerical results of new topologies of beam structure using two nonzero materials (concrete and steel only) and with void and two nonzero materials (void, concrete, and steel) are compared. For the second example, a deep beam structure taken from Goodchild et al. (2014) is presented. The example is meant to demonstrate the feasibility of the ESO method for reinforced concrete structures, i. e., to prove that it is possible to obtain lighter structural elements in an elastic state without reaching the failure surface criterion of any material.

4.1 Corbel joined to a column

The geometry of the first analyzed structure is presented in Figure 1. The following material parameters are used for the steel: $E_1 = 10.0$ and $\nu = 0.30$; concrete: $E_2 = 1.0$ and $\nu = 0.20$; and, the void: $E_3 = \nu = 0$. The number of finite elements used for the discretization of the design domain was 88×216 (19008 elements). The boundary conditions in the model are applied to five nodes on the top part of the column and five nodes on the bottom, restraining both x and y directions.

Since the loads are not to scale, the only relevant factor in choosing the material's stiffness is their ratio. It is used a stiffness ratio between steel and concrete of 10. Besides that, according to de Marco (2018), the magnitude of the absolute concrete's tensile and compressive strength in the procedure are irrelevant, but their proportion is. A relation of tensile strength of concrete between tensile and compression of 0.2 was chosen.

Regarding the ESO method parameters, a penalty exponent applied to the optimization routine $p = 3$ and to the steel cover in the structure $p = 2$ is considered. To obtain the final topology, without violating materials' stress criterion limit, it was necessary to use three optimization cycles (or phases), that is, in each cycle, two materials are chosen for optimization together with a failure criterion. For the first phase, for instance, the algorithm uses the von Mises failure criterion to distribute the volume of steel material and voids for a given value of steel volume fraction stipulated by the designer for that phase. Next, the Ottosen or Drucker-Prager criterion can be used to remove a portion of the steel material,

replacing it with concrete. In the end, at least for the topologies that are presented, a tensile stress criterion is adopted to redistribute the materials to zones subject to compression (concrete) and tension (steel) ensuring adequate concrete cover.

So, the following steel volumes are adopted for each phase: 50%, 35%, and 15%. Also, the parameter of evolutionary ratio (er), to determine the decrease of volume in each phase, are: 4%, 3%, and 2%; and the size of the filter scheme (r_{min}), to avoid checkerboard patterns, are 8, 3, and 2. This is an important parameter to correctly drive the solution for the reinforced concrete designs for the following two reasons: to avoid creating too many slender concrete members and to prevent the removal of very thin but relevant steel parts within concrete. A concrete cover of 2 elements is also imposed.

Therefore, the results of this analysis are shown in Figures 2 and 3 when using the Drucker-Prager and Ottosen criteria, respectively. In Figures 2 and 3, grey represents the concrete, black represents steel and white represents voids.

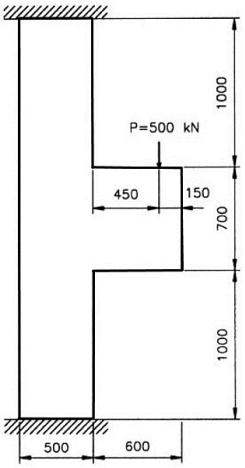

Figure 1 – Loaded corbel joined to a column (Adapted from de Marco, 2018).

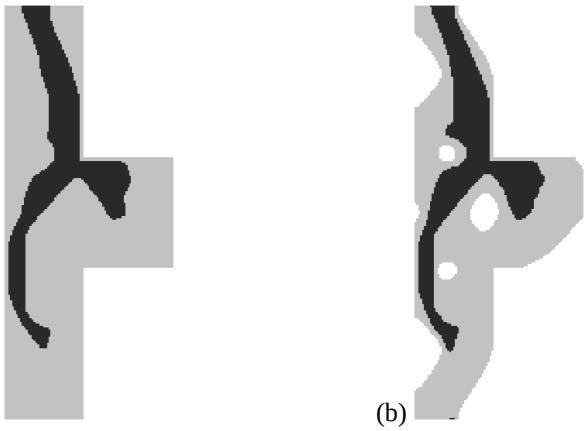

(a) (b)

Figure 2 – Final topology obtained when considering the Drucker-Prager concrete criterion using (a) two-phases with two nonzero materials and (b) three-phases with two nonzero materials.

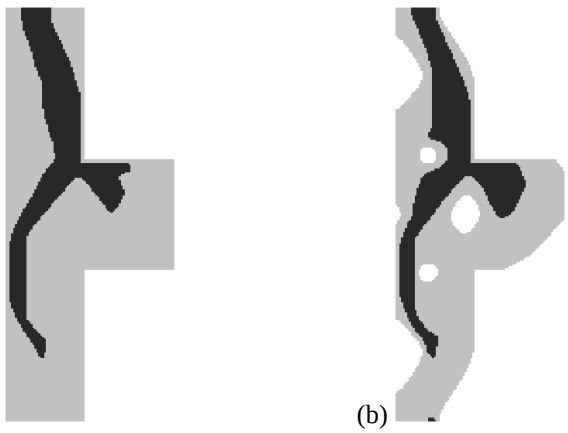

(a) (b)

Figure 3 – Final topology obtained when considering the Ottosen's 4-parameters concrete criterion using (a) two-phases with two nonzero materials and (b) three-phases with two nonzero materials.

As seen in Figures 2 and 3, the final topologies do not show significant distinction in steel material distribution for two-phases and three-phase optimization, regardless of the failure surface criterion used. This demonstrates that for a topological optimization with a stress constraints standpoint, the adopted criterion does not have a significant influence on the final topology. It is expected small differences in the final predicted stress states for different failure criteria. However, depending on the equation adopted to represent the material's failure, this can lead to greater computational processing time, especially if the non-linear analysis is considered.

4.2 Deep beam

The geometry of the second structure is depicted in Figure 4(a). Unlike the first example, this structure considers an actual design for a thick beam made of reinforced concrete. The beam is supported by columns of 600×450mm. Dead and live loads of $G_k = 1256$ kN and $Q_k = 480\ kN$ acting 950 mm from one support are applied on a rigid bearing plate of 450×450 mm. Regarding the materials parameters, it is considered concrete grade C35 and f_{yk} =500 MPa steel, resulting in: $E_1 = 210 \times 10^9$ Pa and $\nu = 0.30$ for the steel rebars; $E_2 = 33 \times 10^9$ Pa and $\nu = 0.20$ for the concrete; and, $E_3 = \nu = 0$ for the voids. Also, the concrete presents a uniaxial compressive strength of 33×10^6 Pa and tensile strength of 3×10^6 Pa (parameters used for the Ottosen criterion). The concrete cover is assumed 25 mm. This beam was calculated using the usual Strut and Tie (ST) methodology according to the Eurocode 2 by Goodchild et al. (2014) and the resulting detailing is presented in Figure 4(b).

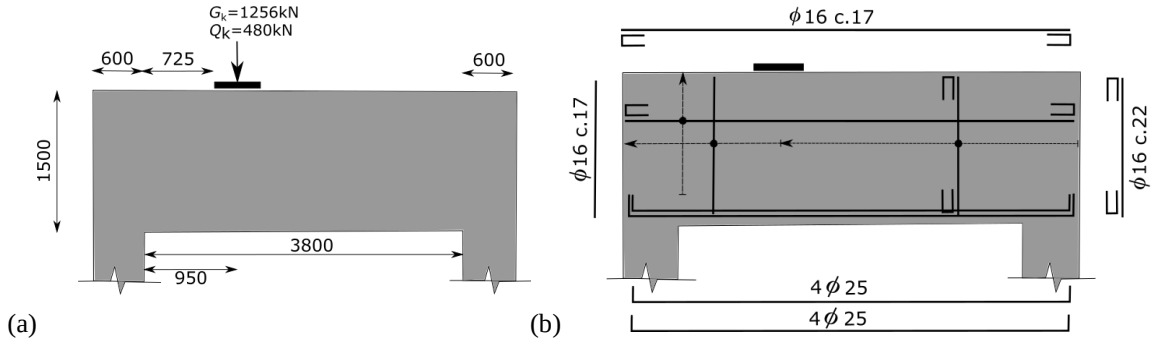

Figure 4 – (a) Deep beam geometry. (b) Reinforcement detailing according to Eurocode2 (Adapted from Goodchild et al., 2014).

Therefore, Figure 5 presents the final topology for the deep beam. Three phases (voids and solids) were assumed. Gray represents concrete and black, steel. In Figure 6, the longitudinal deformation (ε_{xx}) of the topology is presented with bar colors. In addition, the stress distribution considering the von Mises criterion and Ottosen's 4-parameters criterion are shown in Figure 7. For the results obtained, the structure's weight was not considered in the solution but added to the dead load as indicated in Figure 4(a).

Figure 5 – Final topology obtained for Ottosen's 4-parameters concrete criterion/von Mises criterion(steel).

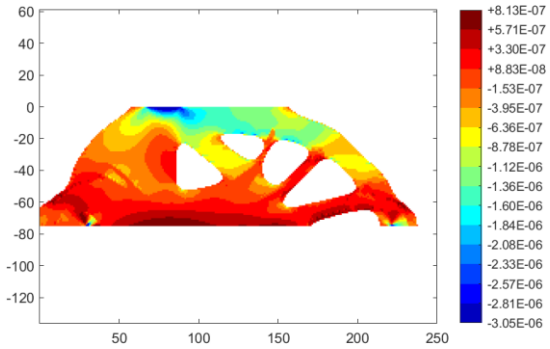

Figure 6 – The deformation in the x direction (ε_{xx}) of the final topology of the deep beam.

Observing Figure 6, it can be seen that the concrete deformation is below the concrete's maximum compressive strength of 3.5‰ (in the color bar, $\varepsilon_{xx} = -3.05 \times 10^{-6}$ m/m) at the upper compressed zone and the left and right inclined struts. The same can be said for the ε_{xx} deformation in the steel (bottom of the beam in Figure 6) which is below the yielding limit of 0.1% and consequently the ultimate strain of 1%.

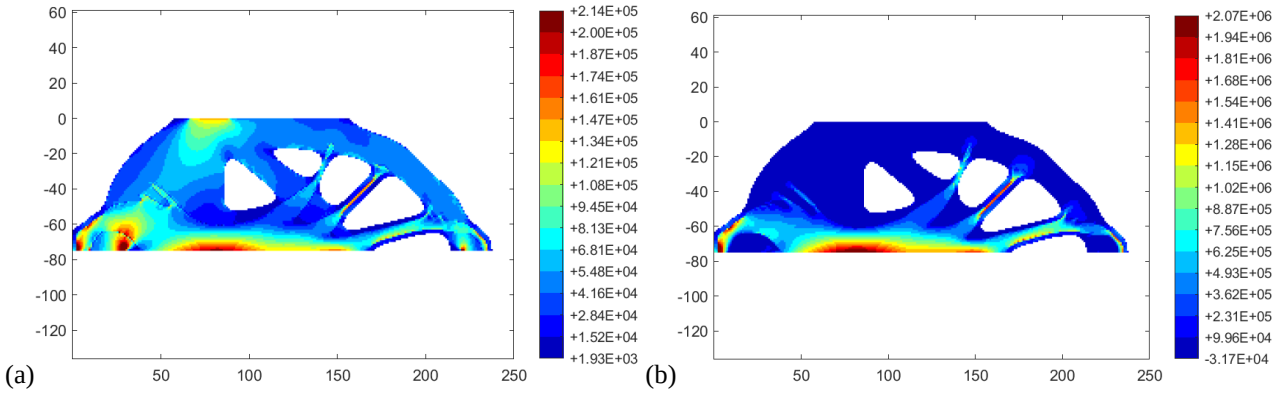

Figure 7 – Stress distribution along with the final topology of the deep beam by the criterion: (a) of von Mises and (b) Ottosen's 4-parameters (Pa).

Taking into consideration the stress distribution, in the Ottosen stress graph, Figure 7(b), and leaving aside the calculated stresses at the points where the reinforcements are present, it is clear that the material is within the specified concrete uniaxial compressive strength $f_{cm} = 33 \times 10^6$ Pa. The von Mises stress graph, Figure 7(a), disregarding the points where there is concrete, indicates a maximum limit in the reinforcement of 0.21 MPa at the bottom face of the beam and close to the support on the left, indicating a value well below the yielding limit that would indicate linear elastic behavior. Thus enabling a reduction in the structure's steel volume. This indicates that the final topology for the beam is below the material failure curves on the stress-strain curve.

Finally, a qualitative assessment between the topology found by the ESO method (Figure 5) and the arrangement of steels addressed by Goodchild et al. (2014) when implementing the strut-and-tie model (Figure 8) will be presented. Comparing the final topology optimized for a stress constraint of a deep beam (Figure 5) with the truss proposed by Goodchild et al. (2014) for the ST model, it is clear that the struts of the right support (member 1-2 and 7-6, Figure 8) have a very close inclination to the optimized in this paper.

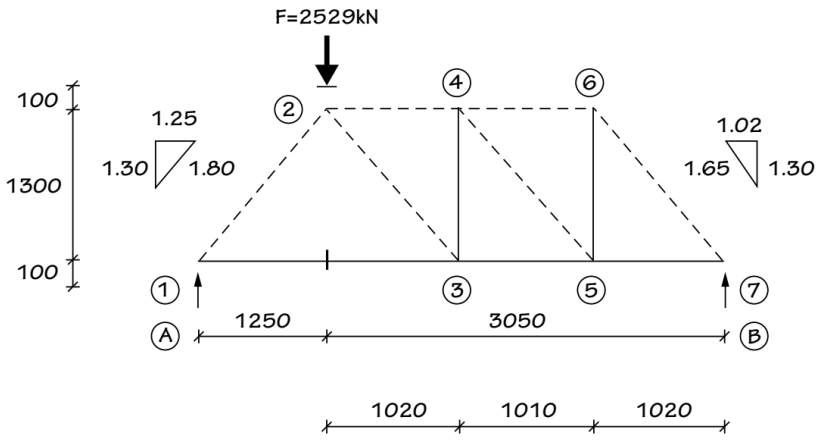

Figure 8 –Strut-and-tie model proposed by Goodchild et al (2014).

However, the optimized model generated three inclined ties (one of them at 45º, as expected) while the ST assumed model resulted in two vertical ties (members 3-4 and 5-6, Figure 8), which is a common solution for stirrups in a practical constructive standpoint.

In addition, it is noteworthy that, from the designer's point of view, when adopting a strut-and-tie model, one must have prior knowledge of how the structures behave so that one can distribute the steel material properly along with the structure. However, when implementing a topological optimization method and also meeting the failure criteria of the materials, this prior knowledge is no longer necessary due to the material reallocation that the algorithm performs. With this, a new frontier is opened for the creation of lighter structures that are different from standard geometries defined by requirement codes.

5. FINAL REMARKS

This paper presented a multi-phase, multi-material topology optimization scheme with stress constraints. Concrete and steel were used as solid elements, and in the examples with three phases, voids were allowed. Failure surface criteria were assumed for concrete (2-parameter Drucker-Prager or 4-parameter Ottosen) and steel (von Mises). Compliance objective function, as well as sensitivity-based failure criteria, were adopted in a three-step topology optimization (*i*) void insertion for minimum steel compliance, (*ii*) steel to concrete change for compression zones, and (*iii*) reduction of steel as much as possible to tensile zones only).

In the first numerical example, a comparison between the Ottosen and Drucker-Prager models were presented to verify how much this choice made by the designer can influence the final topology for the case of a loaded corbel jointed to a column. In this example, illustrative values were used to represent the material properties. The results indicated that the final topologies do not show significant distinctions in the steel material distribution for two-phase and three-phase optimization regardless of the failure surface criterion used.

In the second example, an actual design for a deep beam made of reinforced concrete was brought to be analyzed. Results regarding the stress and strain distribution along the structure were presented. In the final topology, one could notice that the development of lighter structures than those presented in this article is a promising possibility. Furthermore, in this example, a qualitative assessment between the final topology and the strut-and-tie model was performed. At this stage of the analysis, it was observed that the strut-and-tie model has a more practical effect than that obtained by the ESO method. However, the topological optimization method appears to idealize the structures for their best structural performance. Thus, making it possible to obtain lighter structures.

As future work, it is intended to automate the detailing of the reinforcements from the values of the forces acting on the steel elements. Also, for the final optimized structure, a final geometric nonlinear analysis to obtain more accurate results for displacement and deformation are intended to be performed.

6. ACKNOWLEDGEMENTS

The authors thank Brazilian agencies Coordenação de Aperfeiçoamento de Pessoal de Nível Superior (CAPES) and Conselho Nacional de Desenvolvimento Científico e Tecnológico (CNPq) for the support to this research.

7. REFERENCES

Amir, O., 2013. “A topology optimization procedure for reinforced concrete structures”. *Computers and Structures*, Vol. 114-115, pp. 46-58.

Bendsøe, M. P., Sigmund, O., 2003. *Topology optimization: Theory, Methods and applications*. Editora Springer-Verlag, Berlin.

CEB-FIP. Model code 2010, Volume 1. International Federation for Structural Concrete (fib), 2010. fib Bulletin 65.

De Marco, A., 2018. *Application of Evolutionary Structural Optimization to Reinforced Concrete Structures*. Master’s Thesis, Faculty of Civil Engineering and Geosciences, Delft University and Technology, The Netherlands.

Goodchild, C. H., Morrison, J., Vollum, R. L., 2014. *Strut-and-tie Models – How to design concrete members using strut-and-tie models in accordance with Eurocode2*. Ed. MPA The Concrete Centre, London.

Huang, X., Xie, Y. M., 2010. *Evolutionary Topology Optimization of Continuum Structures: Methods and Applications*. Editora John Wiley & Sons Ltd.

Jewett, J. L., Carstensen, J. V., 2019. “Topology-optimization design, construction and experimental evaluation of concrete beams”. *Automation in Construction*, Vol. 102, pp. 59-67.

Li, Y., Xie, Y. M., 2021. “Evolutionary topology optimization for structures made of multiple materials with different properties in tension and compression”. *Composite Structures*, Vol. 259.

Liu, Y., Jewett, J. L., Carstensen, J. V., 2020. “Experimental Investigation of Topology-Optimized Deep Reinforced Concrete Beams with Reduced Concrete Volume”. In *Second RILEM International Conference on Concrete and Digital Fabrication*, pp. 601-611.

Lund, E., 2009. “Buckling topology optimization of laminated multi-material composite shell structures”. *Composite Structures*, Vol. 91, pp. 158-167.

Luo, Y., Wang, M. Y., Zhou, M., Deng, Z., 2012. “Optimal topology design of steel-concrete composite structures under stiffness and strength constraints”. *Computer and Structures*, Vol. 112-113, pp. 433-444.

Oliveira, D. B., Penna, S. S., Pitangueira, R. L. S., 2020. “Elastoplastic constitutive modeling for concrete: a theoretical and computational approach”. *Ibracon Structures and Materials Journal*, Vol. 13, pp. 171-182.

Ottosen, N. S., 1977. “A failure criterion for concrete”. *A Journal of the Engineering Mechanics Division*, Vol. 103, pp. 527-535.

Querin, O. M., Victoria, M., Alonso, C., Ansola, R., Martí, P., 2017. *Topology Design Method for Structural Optimization*. Editora Academic Press.

Sethian, J. A., Wiegmann, A., 2000. "Structural boundary design via level set and immersed interface methods". *Journal of Computational Physics*, Vol. 2, pp. 489-528.

Tong, G., Pengli, X., Weihong, Z., 2016. "Topology optimization of thermo-elastic structures with multiple materials under mass constraint". *Computers and Structures*, Vol. 173, pp. 150-160.

Wang, M. Y., Wang, X., 2004. ""Color" level sets: a multi-phase method for structural topology optimization with multiple materials". *Computer Methods in Applied Mechanics and Engineering*, Vol. 193, pp. 469-496.

Xie, Y. M., Steven, G. P., 1997. *Evolutionary Structural Optimization*. Editora Springer, London.

Zhang, X. S., Chi, H., 2020. "Efficient multi-material continuum topology optimization considering hyperelasticity: Achieving local feature control through regional constraints". *Mechanics Research Communications*, Vol. 105.

7. RESPONSIBILITY NOTICE

The authors are the only responsible for the printed material included in this paper.